

# Analytical Model of the Refrigeration System for Cooling in a Hygroscopic Cycle Power Plant

Roberto Martínez-Pérez<sup>1</sup>, Bernardo Peris-Pérez<sup>2</sup>, Juan Carlos Ríos-Fernández<sup>1</sup>,  
 Juan M. González-Caballín<sup>1</sup>, Francisco Rubio-Serrano<sup>3</sup>, Antonio J. Gutiérrez Trashorras<sup>1</sup>

<sup>1</sup> Department of Energy, University of Oviedo

Escuela Politécnica de Ingeniería, c/ Wifredo Ricart s/n, 33203 - Gijón, Asturias (Spain)

Phone/Fax number: +0034 985 182428, e-mail: [martinezroberto@uniovi.es](mailto:martinezroberto@uniovi.es) (R. Martínez), [riosjuan@uniovi.es](mailto:riosjuan@uniovi.es) (J.C. Ríos), [gonzalezsjuan@uniovi.es](mailto:gonzalezsjuan@uniovi.es) (J. M. González-Caballín), [gutierrezantonio@uniovi.es](mailto:gutierrezantonio@uniovi.es) (A. J. Gutiérrez)

<sup>2</sup> Department of Mechanical, Thermal and Fluid Engineering, Escuela de Ingenierías Industriales

Dr. Ortiz Ramos s/n. 29071 Málaga (Spain)

Phone/Fax number: +0034 951 952399, e-mail: [perisbernardo@uma.es](mailto:perisbernardo@uma.es) (B. Peris)

<sup>3</sup> IMATECH, IMASA Technologies, S.L.U.

St. Carpinteros 12, 28670 Villaviciosa de Odón, Madrid (Spain)

Phone number: +0034 91 781 75 88, email: [fj.rubio@imasa.com](mailto:fj.rubio@imasa.com) (F.J. Rubio)

## Abstract.

The Hygroscopic Cycle is an innovative power cycle due to the significant energy and water consumption savings it allows. The cycle is currently in the improvement study phase. In this work, the refrigeration process of the cycle has been analyzed using dry-coolers and without the need to consume water, which confers a significant environmental and energy efficiency improvement of the process. The numerical study of the refrigeration of the Hygroscopic Cycle was carried out to improve its understanding and performance in order to obtain optimal results. A model of the equipment was first implemented using the Engineering Equation Solver software. Once modeled, the system was analyzed for different situations and working conditions and validated using the real data provided by the first power pilot plant that uses this cycle. That made it possible to design specific equipment that would respond to the needs of any installation that used the Hygroscopic Cycle.

## Key words.

Hygroscopic cycle; Electrical efficiency; Dry-cooler; Cooling water saving.

## Nomenclature.

$A$ : heat transfer area

$A_{fins}$ : fins area

$D_i$ : inside diameter of tubes

$D_o$ : outside diameter of tubes

$error_T$ : error in temperatures

$Eu$ : Euler number

$F$ : correction factor

$L$ : total length of tubes

$LMTD$ : mean logarithmic temperature difference

$L_M$ : tube height

$L_{tube}$ : length of each tube

$N$ : number of tube columns

$N_{fins}$ : number of fins

$Pr$ : Prandtl number

$\rho_h$ : hot fluid density

$\rho_c$ : cold fluid density

$\dot{Q}$ : heat transfer rate

$Re$ : Reynolds number

$Re_c$ : Reynolds number of the cold fluid

$Re_h$ : Reynolds number of the hot fluid

$r_o$ : outer radius of the tubes

$r_{fins}$ : fins radius

$S_D$ : diagonal distance between tubes

$S_P$ : space between tips

$S_L$ : longitudinal distance between tubes

$S_T$ : transverse distance between tubes

$T_a$ : ambient temperature

$T_c$ : average cold fluid temperature

$T_{ci}$ : cold fluid inlet temperature

- $T_{co}$ : cold fluid outlet temperature
- $t_{fins}$ : fins thickness
- $T_{hi}$ : hot fluid inlet temperature
- $T_{ho}$ : hot fluid outlet temperature
- $U$ : global heat transfer coefficient
- $\mu_h$ : dynamic viscosity of hot fluid
- $v_h$ : velocity of hot fluid
- $v_c$ : velocity of cold fluid
- $\dot{V}_h$ : volume flow rate of hot fluid
- $\dot{V}_c$ : volume flow rate of cold fluid
- $W_e$ : electrical power of the fans
- $W_m$ : fan mechanical power
- $\Delta P_h$ : hot fluid pressure drop
- $\Delta P_c$ : cold fluid pressure drop
- $\eta_{fins}$ : fin efficiency
- $\eta_{fan}$ : fan efficiency

## 1. Introduction

The Hygroscopic Cycle (HC) has similar characteristics to the Rankine Cycle (RC). However, this new technology is characterized by working with hygroscopic components [1]. The hygroscopic compounds are capable of absorbing water in the form of vapor or liquid state and must have a vapor pressure lower than that of water and be easily separable; that is, the process can be reversed [2]. In addition, hygroscopic compounds must be chemically stable for the working pressures and temperatures of the cycle, being, in turn, non-flammable and non-toxic. Furthermore, The HC can be used in different power plants in which the objective is to obtain electrical energy. Unlike the RC, which uses a condenser, an absorber is used in the HC. Thanks to the absorption capacity of hygroscopic solutions, condensation by absorption occurs in the absorber.

A pilot plant located in Asturias (Spain) reproduces the HC for both low and high hygroscopic compounds concentration [3], [4]. The boiler has a nominal power of 100 kW and the fuel is natural gas. That boiler is able to produce 110 kg/h of steam. The plant does not have a conventional steam turbine. The turbine is replaced by an expansion valve which accurately simulates the processes carried out by a turbine using a Supervisory Control and Data Acquisition (SCADA) system. The layout of the pilot plant and its main components are represented in Figure 1.

The valve conditions that replace the turbine were 60 bar and 500 °C (at the inlet of the valve). The flow that comes out of this valve goes to the steam absorber, where it is mixed with the cooling reflux, which is a solution of water and hygroscopic compounds. The condensed fluid at the exit of the absorber is also a solution of water and hygroscopic compounds.

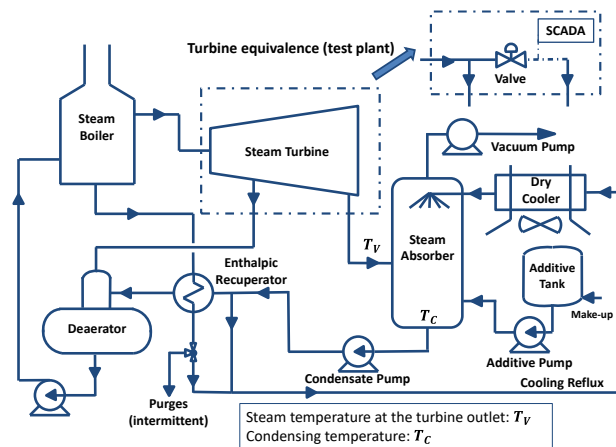


Fig. 1. Diagram of the pilot plant with HC [3], [5]

The condensed fluid at the exit of the absorber is also a solution of water and hygroscopic compounds. The temperature  $T_C$  represented the condensing temperature and  $T_V$  the saturation temperature of the turbine steam at the same pressure.  $T_C$  is always greater than  $T_V$  due to the absorption process. Part of the condensed flow is propelled to the deaerator and the rest is recirculated and refrigerated. After the deaerator, the flow is directed towards the boiler.

Figure 2 shows the biomass plant at an industrial scale with HC incorporated and located in Córdoba. That plant works with low concentration of hygroscopic compounds (lower than 0.01%). The steam coming out of the turbine (1) is introduced into the absorber, joining it with a solution of water (2) and hygroscopic compounds with a higher conductivity than that of steam. The absorber is connected to vacuum pumps [6] which maintain the vacuum level both at the beginning of the process and throughout the operation time. These pumps are small, therefore, consume much less energy than that consumed by a conventional RC condenser [7]. In the absorber, a condensing temperature higher than the saturation temperature of pure vapor is reached at a given pressure. The condensed fluid (3) comes out of the absorber and is propelled toward two circuits. One of them goes to the deaerator (4), where oxygen and other non-condensable gases are removed. The other part of the condensed flow is directed towards the air coolers (dry-coolers) (2), where the cycle is refrigerated and the heat is released to the ambient. One of the conditions met by incorporating the HC is to work with the lowest pressure supported by the turbine, always maintaining maximum electricity production and increasing the cooling temperature. The flow that comes out of the deaerator is driven into the boiler and is subsequently introduced into the turbine, closing the cycle. The thermal energy from the boiler purges (5) is recovered by means of an enthalpy recuperator, transferring its energy to the flow that enters the deaerator. This energy recovery is one of the keys to the proper functioning of the cycle. In addition, a part of the purges from the boiler (6) is intermittently eliminated from the system in order to maintain a chemical balance in the circuit due to the steam losses that usually occur in all power cycles.

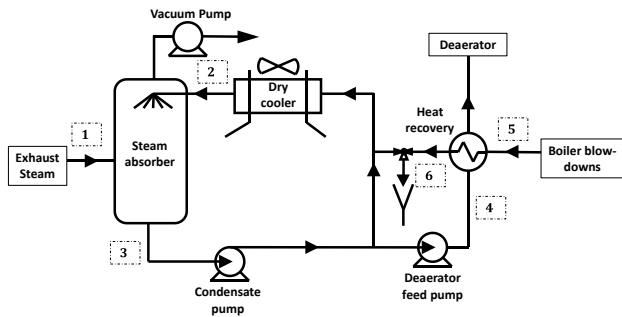


Fig. 2. HC process diagram in a plant located in Cordoba (Spain) [5].

According to [5], for the same condensing pressure, the cooling temperature is 13 °C higher in a real HC than in Rankine Cycle at an industrial scale. For this reason, cooling solely by air is possible in this cycle since there is enough difference between the hot fluid and the air temperatures. The average condensing pressure of HC is 0.186 bar. With this pressure, the refrigeration temperature in the RC is 31 °C, while for the HC it is 44 °C.

For the same ambient temperatures, the electrical energy consumption of the dry-coolers is much higher in the RC than in the HC. On the other hand, in 2018 Rubio-Serrano et al. verified that, from a temperature of 27 °C, the RC begins to consume water through cooling towers, while, in the HC, it can work with ambient temperatures up to 40 °C without consuming water [5].

The following gap was identified: there were no publications on the dry-coolers used in the HC and that would require a more specific design to enhance the dissipation of large amounts of thermal power.

The objective of the study was to develop an analytical model that would allow knowing in detail about the configuration and internal functioning of the HC dry-cooling system.

## 2. Methodology

The EES software [8] has been used for developing the model of the dry-coolers. It was verified experimentally in the pilot plant that when solutions with very low concentrations of hygroscopic compounds (< 0.01%) were used, the properties of the solution were close to those of pure water. The model was developed for concentrations less than 0.01% and therefore, the properties of pure water were used for dissolution.

When analyzing this heat exchanger, the Logarithmic Mean Temperature Difference (LMTD) method was used. This method provides us with a formula that defines the thermal power (4). In it, LMTD represents the average temperature difference between the two working fluids. Apart from the global heat transfer coefficient (U) and the heat transfer area (A), a variable F appears. This variable is a correction factor used when the heat exchanger is designed for crossflow.

$$Q = LMTD \cdot U \cdot A \cdot F \quad (1)$$

The LMTD value is calculated by equation (2). In addition, to calculate the correction factor F, the formulas from (3) to (6) are used [9].

$$LMTD = \frac{(T_{hi}-T_{co})-(T_{ho}-T_{ci})}{\ln\left(\frac{T_{hi}-T_{co}}{T_{ho}-T_{ci}}\right)} \quad (2)$$

$$F = \frac{\ln\left(\frac{1-R \cdot P}{1-P}\right)}{NTU \cdot \left(\frac{1}{R}-1\right)} \quad (3)$$

$$NTU = -R \cdot \ln\left(1 + \frac{\ln(1-R \cdot P)}{R}\right) \quad (4)$$

$$P = \frac{T_{ho}-T_{hi}}{T_{ci}-T_{hi}} \quad (5)$$

$$R = \frac{T_{ci}-T_{co}}{T_{ho}-T_{hi}} \quad (6)$$

### A. Convection heat transfer coefficient on the outside of the tubes

To calculate the convection heat transfer coefficient on the outside of the exchanger tubes, the Briggs and Young correlation [10] was used. This correlation is reflected in equation (7).

$$Nu_c = 0.134 \cdot Re_c^{0.681} \cdot Pr_c^{1/3} \cdot \left(\frac{r_{fins}-r_o}{s_f}\right)^{-0.2} \cdot \left(\frac{t_{fins}}{s_f}\right)^{-0.1134} \quad (7)$$

Equation (8) was used to calculate the Reynolds number. However, the speed needed to calculate the Reynolds, in our case, was the maximum between equations (9) and (10) [11]. To calculate the speed, it was necessary to use equation (11), which represents the speed of the air just before entering between the tubes. The value of the diagonal distance between tubes was obtained with equation (12).

$$Re_h = \frac{v_h \cdot \rho_h \cdot D_i}{\mu_h} \quad (8)$$

$$v_c = \frac{S_T}{S_T - D_o} \cdot v_{initial} \quad (9)$$

$$v_c = \frac{S_T}{2(S_D - D_o)} \cdot v_{initial} \quad (10)$$

$$v_{initial} = \frac{\dot{V}}{L_{tube} \cdot L_M} \quad (11)$$

$$S_D = \sqrt{\left(\frac{S_T}{2}\right)^2 + S_L^2} \quad (12)$$

As in the previous case, the thermal properties of the air were evaluated at the average temperature between the inlet and outlet temperatures, represented in equation (13).

$$T_c = T_{ci} + T_{co} \quad (13)$$

Equation (14) represents the thermal power absorbed by the air, while equation (15) represents the thermal power transferred by the liquid fluid.

$$\dot{Q} = \dot{m}_c \cdot cp_c \cdot (T_{co} - T_{ci}) \quad (14)$$

$$\dot{Q} = \dot{m}_h \cdot (h_{hi} - h_{ho}) \quad (15)$$

### B. Pressure drop in airflow

To calculate the pressure drop produced on the outside of the tubes, and therefore the pressure drops in the air, equation (16) was used.

$$\Delta P_c = Eu \cdot \rho_c \cdot v_c^2 \quad (16)$$

To calculate this pressure drop, it was necessary to know the value of the Euler number. For this, the Robinson and Briggs correlation [12] was used, which is presented in equation (17).

$$Eu = 18.93 \cdot Re_f^{-0.316} \cdot \left(\frac{S_r}{D_e}\right)^{-0.927} \cdot \left(\frac{S_r}{S_D}\right)^{0.515} \cdot N \quad (17)$$

### C. Power consumed by the fans

Once the pressure drop outside the tubes was calculated, it was possible to calculate the mechanical power that the fans had to supply. Once this mechanical power was calculated and knowing the efficiency of the fans, it was possible to obtain the electrical power consumed by them. Equation (50) represents the calculation of mechanical power. On the other hand, equation (51) represents the electrical energy consumed by the fans.

$$W_m = \Delta P_c \cdot \dot{V}_c \quad (18)$$

$$W_e = \frac{W_m}{\eta_{fan}} \quad (19)$$

### D. Model parameters

The specific parameters of the model developed are detailed in Table 1.

Table 1. Parameters of the analytical model

Pipe length (m)	5.67
Tube diameter (mm)	12
Tube material	Copper
Fins thickness (mm)	0.2
Fin pitch (mm)	2.2
Fin material	Aluminum
$A_{total}$ (m <sup>2</sup> )	1,023.12
$A_{fins}$ (m <sup>2</sup> )	984.48
L (m)	1,132.95
$N_{fins}$	539,500
$r_{fins}$ (m)	0.018
$\eta_{fan}$ (%)	70

### E. Simulations

The analytical model has been successfully validated in other similar applications [13]. In this case, the model made in EES was used for the simulation of the dry-coolers under the following two sets of initial working conditions:

- Setting the inlet temperature of the hot and cold fluids and the outlet temperature of the hot fluid.
- Setting the inlet temperature of the hot and cold fluids and the fluid flow of the hot fluid.

### F. Experimental contrast

Experimental validation was achieved by defining four cases with different boundary condition values. In this sense, experimental data was gathered in the pilot plant for four different ambient temperatures ( $T_a$ ) respectively (Table 2). This information was used to contrast the values obtained in the simulations and to validate the model.

## 3. Results

Experimental data obtained in the pilot plant for the different cases with different fixed ambient temperatures are detailed in Table 2. The nominal power of the fans in the pilot plant was 3 kW. This power was important since the design had to ensure that the electrical power consumed was always below this value.

Table 2. Experimental data obtained for the four cases.

	Case 1	Case 2	Case 3	Case 4
$T_a$ (°C)	10.02	17.84	24.15	35.10
$T_{hi}$ (°C)	25.15	33.62	33.91	50.90
$T_{ho}$ (°C)	18.10	26.31	32.60	43.91
$\dot{V}_h$ (m <sup>3</sup> /h)	18.00	18.05	18.06	18.06
$\dot{V}_c$ (m <sup>3</sup> /h)	51,239.8	51,240.0	51,240.2	51,240.3
$W_e$ (kW)	2.36	2.36	2.37	2.37

With all the equations and variables presented, the detailed calculation of the dry-coolers was possible. The resulting values will be presented below in the four different cases for which data provided by the pilot plant. The comparison of these results helped to contrast the design to later extrapolate the results to other working conditions. Once the heat exchanger was designed, the results could be compared with the available data.

It should be noted that, for the different cases, the input variables are the mass flow rates of both fluids and their inlet temperatures. The following two sets of simulations were made.

#### A. Setting the inlet temperature of the hot and cold fluids and the outlet temperature of the hot fluid

Setting the inlet temperature of the hot and cold fluids and the outlet temperature of the hot fluid, we obtained the results reflected in Table 3.

Table 3. Simulation results setting the inlet temperature of the hot and cold fluids and the outlet temperature of the hot fluid

	Case 1	Case 2	Case 3	Case 4
$T_{hi}$ (°C)	25.15	33.62	39.91	50.90
$T_{ho}$ (°C)	18.10	26.31	32.60	43.91
$T_{ci}$ (°C)	10.02	17.84	24.15	35.10
$T_{co}$ (°C)	18.00	26.95	34.06	44.22
$\dot{V}_h$ (m <sup>3</sup> /h)	18.00	18.10	18.70	18.80
$\dot{V}_c$ (m <sup>3</sup> /h)	51,238.3	51,238.9	51,239.2	51,239.9
$U$ (W/ m <sup>2</sup> K)	25.10	25.31	25.66	26.13
$F$	0.81	0.81	0.8	0.8
$\eta_{fins}$	86.10	86.13	86.21	86.36
$\dot{Q}$ (kW)	139.00	139.08	139.35	139.90
$W_e$ (kW)	2.37	2.38	2.38	2.39

**B. Setting the inlet temperature of the hot and cold fluids and the fluid flow of the hot fluid**

Setting the inlet temperature of the hot and cold fluids and the fluid flow of the hot fluid, we obtained the results reflected in Table 4.

Table 4. Simulation results setting the inlet temperature of the hot and cold fluids and the fluid flow of the hot fluid

	Case 1	Case 2	Case 3	Case 4
$T_{hi}$ (°C)	25.15	33.62	39.91	50.90
$T_{ho}$ (°C)	18.50	26.87	32.89	44.10
$T_{ci}$ (°C)	10.02	17.84	24.15	35.10
$T_{co}$ (°C)	18.90	26.69	33.83	44.56
$\dot{V}_h$ (m <sup>3</sup> /h)	18.00	18.05	18.06	18.06
$\dot{V}_c$ (m <sup>3</sup> /h)	51,238.1	51,239.0	51,240.0	51,241.2
$U$ (W/ m <sup>2</sup> K)	25.30	25.31	25.66	26.13
$F$	0.81	0.81	0.81	0.80
$\eta_{fins}$	86.10	86.13	86.21	86.36
$\dot{Q}$ (kW)	140.07	141.32	141.88	141.91
$W_e$ (kW)	2.39	2.40	2.41	2.41

**C. Experimental contrast**

The results of the errors for simulations A and B are included in Figure 4 and 5.

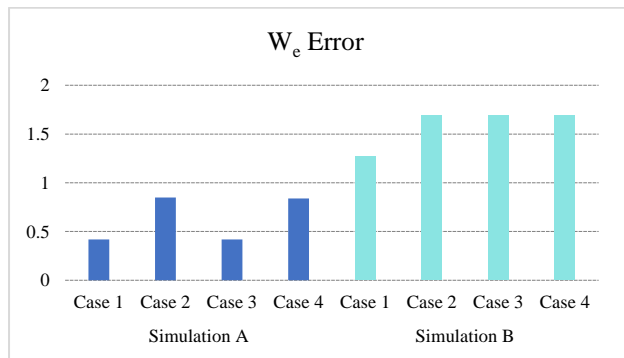


Fig. 3. Error in the value of nominal power of the fans with simulations A and B.

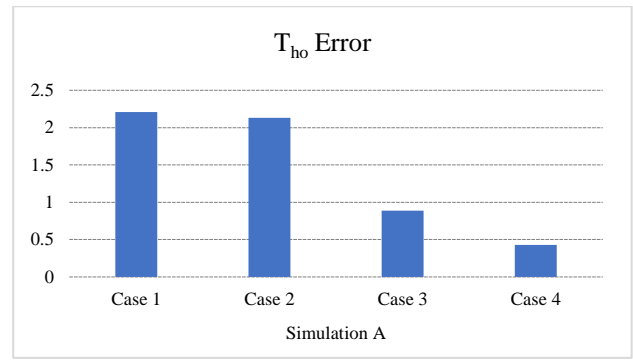


Fig. 4. Error in the value of the outlet temperature of the hot fluid with simulation A.

According to the results, errors obtained are lower than 2 % for the value of power consumption of the fans and lower than 2.5 % for the value of the outlet temperature of the hot fluid, which allows us to validate the design. These results allowed us to contrast the design to later extrapolate the results to other working conditions.

**4. Conclusions**

The model developed for the simulation of the dry-coolers has been validated with the experimental results obtained in the pilot plant.

The model of the dry system for the refrigeration of the HCT will be very useful for the development of a global model of the cycle and for the simulation under different working conditions. That will, be done in future works in order to improve the efficiency and the general performance of the technology.

**Acknowledgments**

This work has been supported by the project "Improvement of energy performance of the Hygroscopic Cycle for power production" PID2019-108325RB-I00/AEI/10.13039/501100011033 from the Agencia Estatal de Investigación - Ministerio de Ciencia e Innovación, Spain; and "Severo Ochoa" grant program for training in research and teaching of the Principality of Asturias - Spain (BP20-176). The authors also want to acknowledge the contribution of the Spanish company IMATECH (Imasa Technologies), owner of the Hygroscopic cycle pilot plant, as well as the support from the University Institute of Industrial Technology of Asturias (IUTA), financed by the City Council of Gijón, Spain.

## References

- [1] B. Svenningsson, J. Rissler, E. Swietlicki, M. Mircea, M. Bilde, M.C. Facchini, T. Rosenørn, “Hygroscopic growth and critical supersaturations for mixed aerosol particles of inorganic and organic compounds of atmospheric relevance”, *Atmospheric Chemistry and Physics* (2006). Vol. 6 (7), pp. 1937–1952.
- [2] S. Prachayawarakorn, S. Soponronnarit, S. Wetchacama and D. Jaisut, “Desorption isotherms and drying characteristics of shrimp in superheated steam and hot air”, *Drying Technology* (2002). Vol. 20 (3), pp. 669–684.
- [3] F. J. Rubio-Serrano, F. Soto-Pérez and A.J. Gutiérrez-Trashorras, “Experimental study on the influence of the saline concentration in the electrical performance of a Hygroscopic cycle”, *Applied Thermal Engineering* (2020). Vol. 165, pp. 114588.
- [4] Rubio-Serrano, F. J., Soto-Pérez, F. and Gutiérrez-Trashorras, A. J. “Influence of cooling temperature increase in a hygroscopic cycle on the performance of the cooling equipment”, *Energy Conversion and Management* (2019). Vol. 200, pp. 112080.
- [5] F. J. Rubio-Serrano, A. J. Gutiérrez-Trashorras, F. Soto-Pérez, E. Álvarez-Álvarez and E. Blanco-Marigorta, “Advantages of incorporating Hygroscopic Cycle Technology to a 12.5-MW biomass power plant”, *Applied Thermal Engineering* (2018). Vol. 131, pp. 320-327.
- [6] K. Jousten, *Handbook of Vacuum Technology*, Wiley-VCH Verlag DmbH, Weinheim, Germany (2016).
- [7] N. Petchers, *Combined heating, cooling & power handbook: technologies & applications: an integrated approach to energy resource optimisation*, The Fairmont Press Inc, Gistrup, Denmark (2003).
- [8] EES. *Engineering Equation Solver*. Academic Commercial V10.092-3D.
- [9] S. M. Jeter, “Effectiveness and LMTD correction factor of the cross flow exchanger: a simplified and unified treatment”, *ASME Southeast Section Conference* (2006). Vol. 1, pp. 1-10.
- [10] A. Nir, “Heat transfer and friction factor correlations for crossflow over staggered finned tube banks”, *Heat Transfer Engineering* (1991). Vol. 12 (1), pp. 43-58.
- [11] F. P. Incropera and D. P. DeWitt, *Fundamentos de transferencia de calor*, Prentice Hall Hispanoamericana S.A. Naucalpan de Juárez, Mexico (1999).
- [12] M. S. Mon, *Numerical investigation of air-side heat transfer and pressure drop in circular finned-tube heat exchangers*, Technische Universität Bergakademie Freiberg, Germany (2003).
- [13] J.A. Expósito Carrillo, I. Gomis Payá, B. Peris-Pérez and F.J. Sánchez de La Flor, “Air-cooled condensers optimization for novel Ultra-Low Charge ammonia chillers to achieve competitive packaged units”, *Applied Thermal Engineering* (2023). Vol. 219, pp. 119347.